STRESS DISTRIBUTION AND FLEXIBILITY OF THE SUCTION BEND OF THE PRIMARY SODIUM/PUMP LMFBR — SNR 300

H. K. KWEE

Stork Boilers, P.O. Box 20, Hengelo (o), The Netherlands

SUMMARY

Hydrodynamic aspects lead to the design of a special smooth suction bend for the primary sodium pump LMFBR-SNR 300. This bend is built up from two symmetrical halves, formed from plates by explosive forming. To investigate the linear elastic stress distribution and flexibility of this bend for mechanical loads, analyses are made based on two different methods:

First method: The bend is schematized by various toroidal segments with bend parameter λ ranging from 0.049 to 0.22. Each segment is analysed as follows:

Internal pressure: Stress analyses are made using KSHEL computer program developed by Kalnins and based on his theory in [2].

In- and out-of-plane bending: Based on the energy equations developed by von Karman [3] and Vigness [4], theoretical solution is developed by Rodabaugh and George [9] Applying the principal of least work gives the following equation:

$$\left[D(\lambda,r,p,n,E)\right] \left\{c_n\right\} = \left\{-3,\ 0,\ 0,\ 0,\ \text{-----}\right\}^T$$

where D is a symmetrical bandmatrix and c_n is the modified unknown coefficient of the trigoniometric series of the displacement field. The stresses and flexibility could be determined by substituting c_n in the appropriate equations. The membrane circumferential stress distribution obtained by Rodabaugh and George is modified by Dodge and Moore [6] based on the Gross's solution [8].

Computer program PIPEBEND based on the above mentioned solutions is developed for calculating the stresses and flexibility of each toroidal segment.

The second method deals with three dimensional stress analysis. This is necessary to investigate the influence of change of curvatures and cross sections (neglected in the first method). Modelling is done for the symmetry one half of the complete suction bend, applying the thick shell element QUABC9 of the ASKA system. Application of this element for thin shell problems requires reductions of number of integration points. For the considered modal 2x2 reduced integration scheme is chosen only for the transverse shear component.

The results of both methods are compared.

1. Introduction

One of the important aspects of the optimum design of the primary sodium pump for the LMFBR-SNR 300 is the uniform velocity distribution of the sodium in the inlet of the pump. This leads to the design of a special smooth suction bend as shown in fig. 1. This bend is built up from two symmetrical halves, formed from plates by explosive forming.

From an integrity point of view, the design of such a special bend is more complicate than the design of a simple smooth bend with constant cross section. For the nuclear piping system design, the ASME Boiler and Pressure Vessel Code - Section III [1] gives formulas for the simplified stress analyses by using the stress indices and flexibility factors. The application of these formulas to predict the stresses and flexibility of the considered suction bend does not guarantee the reliability of the results. To achieve a more accurate prediction of the stresses and flexibility of that suction bend, linear stress analyses are made based on two different methods.

The first method: The suction bend is schematized by various toroidal segments as shown in Fig. 1. The bend parameter λ of these segments varies in the range from 0.049 to 0.22. By neglecting the end effects of each segments, the stresses and flexibility are predicted by analysing each of the segment. Taking into account that the considered bend parameter can be classified as small, the following analyses are made.

In the case of internal pressure loading stress analyses are carried out using the computer program KSHEL developed by Kalnins based on his theory in [2]. For in-plane and out-of-plane bending of a smooth thin bend with circular cross section, investigation into the stress distribution and flexibility have been made by many authors. In the case of in-plane and out-of-plane bending of large bend-radius bends theoretical solutions were developed by von Karman [3] and Vigness [4] respectively. The theoretical and experimental results were compared by many investigators [5, 6, 9] and for short bend-radius bends by Pardue/Vigness [7] and Gross [8]. Rodabaugh and George [9] developed a theoretical method applicable to a wide range of bend parameter. For the design code purpose Dodge and Moore [6] developed new approximate equations for the stress indices and flexibility factors. Their solutions are based on the Rodabaugh/George's solution and the modified circumferential stress distribution introduced by Gross [8].

For the considered special suction bend application of the Rodabaugh/George's solution combined with Gross's modification for the circumferential stress distribution will in the opinion of the author give the best prediction of the stresses and flexibility. A computer program PIPEBEND based on these solutions is developed for the analyses.

The second method deals with the three dimensional stress analyses of the whole suction bend based on the finite element method. These analyses are necessary to investigate the influences of change in cross section and curvature in the meridional direction. These effects are neglected in the first method. The analyses are carried out using the computer program ASKA.

Comparisons of the results of both methods are made.

2. First method

2.1. Internal pressure: Stress analyses are carried out using the computer program KSHEL. The numerical results of cross sections 2 and 3 are represented in Fig. 4. The positions of the cross sections is given in Fig. 1.

2.2. In-plane and out-of-plane bending: Summary of the theoretical solution developed by Rodabaugh/George combined with Gross's modification for the circumferential stress distribution is given below.

Displacements

The circumferential displacement of the bend wall is assumed as a trigoniometric series expression.

In-plane bending: $v = \sum a_n \text{Sin } 2n\theta$

Out-of-plane bending: $v = \sum a_n \text{Cos } 2n\theta$ eq. (1)

Further, with the assumption of the inextensibility of the middle surface in the circumferential direction, which implies that the circumferential membrane strain $\varepsilon_{\theta m} = 0$, one obtains: $w = - dv/d\theta$ where w is the radial displacement of the bend wall.

Strains

The longitudinal and circumferential strains are given by the following equations:

In-plane bending: $\varepsilon_\phi = (\Delta\alpha/\alpha\ r\text{Sin } \theta + v\text{Cos } \theta + w\text{Sin } \theta)/R$ eq. (2)

Out-of-plane bending: $\varepsilon_\phi = (R/\rho\ r\text{Cos } \theta + v\text{Cos } \theta + w\text{Sin } \theta)/R$ and

for both kinds of bending: $\varepsilon_\theta = \pm t(d^3v/d\theta^3 + dv/d\theta)/2(1-\mu^2)r^2$ eq.(3)

Energy equation

Expressed in the unknown coefficients a_n the total strain energy in a unit of bend length is given by the equation:

$$U = \pi rtE/2R^2\{r^2\eta^2 + 3r\eta a_1 + 9/4a_1^2 + \tfrac{1}{2}\sum a_n^2(1-2n)^2 - 2a_n a_{n+1}(2n-1)(2n+3) + a_{n+1}^2(2n+3)^2 + \lambda^2/12\sum a_n(8n^3-2n)^2 + 4\psi\sum n^2(4n^2-1)a_n^2\}$$ eq. (4)

where $\eta = \Delta\alpha/\alpha$ and $= R/\rho$ for in-plane and out-of-plane bending respectively, $\psi = PR^2/Ert$ and λ is the bend parameter defined as $Rt/r^2\sqrt{1-\mu^2}$

Determination of the coefficients a_n

To determine the values of the coefficients a_n of the displacement functions the principle of least work in used.

$$\partial U/\partial a_n = 0$$ eq. (5)

Performing of this partial differentiation gives the following equations:

$$-\tfrac{1}{2}(2n-3)(2n+1)a_{n-1} + \{(4n^2+1)+(8n^3-2n)^2\lambda^2/6 + 8n^2(4n^2-1)\psi\}a_n - \tfrac{1}{2}a_{n+1}(2n-1)(2n+3) = 0$$ eq. (6)

for $n = 1$: $3r\eta + (5+6\lambda^2+24\psi)a_1 - 5/2\ a_2 = 0$

By introducing the relation $c_n = a_n/r\eta$, eq. (6) can be transformed into the matrix notation given below

$$[D(\lambda, \psi, n)]\{c_n\} = \{-3\ \ 0\ \ 0 - - - \}^T$$ eq. (7)

Flexibility factor

The flexibility factor k is defined by

$$k = EI\eta/MR$$ eq. (8)

where I is the cross-sectional moment of inertia and M is the applied bending moment.

The flexibility factor can be derived by equating the minimized strain energy as defined by eq. (4) to the work done by the bending moment as defined by

$$U_o = \tfrac{1}{2}M\eta/R$$ eq. (9)

From equations (4), (8) and (9) one obtains:

$$k = \{1+3c_1+9/4c_1^2+\tfrac{1}{2}\sum c_n^2(1-2n)^2-2c_n c_{n+1}(2n-1)(2n+3)+c_{n+1}^2(2n+3)^2 + \lambda^2/12\sum c_n^2(8n^3-2n)^2 + \psi\sum 4n^2(4n^2-1)c_n^2\}^{-1}$$ eq. (10)

Stresses

Using the appropriate stress-strain relations and the Gross's solution for determining the circumferential stress, the stresses are given by

In-plane bending : $\sigma_\phi = kMr/I(1-\mu^2)\{X\sin\theta+\frac{1}{2}\sum Y_n \sin(2n+1)\theta \pm \frac{1}{2}\mu\lambda\sum Z_n \cos 2n\theta\}$

$\sigma_\theta = kMr/I(1-\mu^2)\{-1/\gamma\left[X\cos\theta+\frac{1}{2}\sum Y_n/2n+1\cos(2n+1)\theta\right] \cos\theta \pm \frac{1}{2}\lambda\sum Z_n \cos 2n\theta\}$ eq. (11)

Out-of-plane bending : $\sigma_\phi = kMr/I(1-\mu^2)\{X\cos\theta+\frac{1}{2}\sum Y_n \cos(2n+1)\theta \pm \frac{1}{2}\mu\lambda\sum -Z_n \sin 2n\theta\}$

$\sigma_\theta = kMr/I(1-\mu^2)\{1/\gamma\left[X\sin\theta+\frac{1}{2}\sum Y_n/2n+1\sin(2n+1)\theta\right] \sin\theta \pm \frac{1}{2}\lambda\sum -Z_n \sin 2n\theta\}$ eq. (12)

where $X = 1+1.5c_1$; $Y_n = c_n(1-2n)+c_{n+1}(2n+3)$; $Z_n = c_n(2n-8n^3)$; $\gamma = R/r$; σ_ϕ and σ_θ are the longitudinal and circumferential stress respectively.; the plus and minus sign apply to the outside and inside-wall surface respectively.

To calculate the stress distribution and flexibility of each toroidal segment computer program PIPEBEND based on the above mentioned equations has been developed.

Numerical results

To obtain convergence in the solutions ten terms of the trigoniometric series of the displacement are used in the analyses. Presentation of the results is given in the form of distribution of the stress intensification factor $S = \sigma/\sigma_{ob}$ where σ is the actual stress and $\sigma_{ob} = Mr/I$ is the bending stress due to the net bending moment at a cross section. Numerical results for the cross sections 1, 2, 3 and 4 are shown in Fig. 5 to 8.

2.3. The flexibility of the suction bend : The flexibility of the suction bend can be derived if the deformations and rotations at the suction bend's end are known. Prediction of these deformations and rotations is achieved by modelling the suction bend as an assembly of four curved beams with circular cross sections shown in Fig. 2. Due to the deformation of the cross section of the bend, modification of the flexural rigidity of each curved beam is needed. The modified flexural rigidity is given by $EI_o = EI/k$ where k is the flexibility factor as defined in eq. 10, I and I_o are the normal and modified cross-sectional moment of inertia respectively. For torsion loading it is assumed that the torsional rigidity GJ in bar theory is not affected by the deformation of the cross section of the bend. The deformations and rotations at the bend's end are derived by calculating first the end deformations and rotations of each curved beam and then combining them by the method of superposition. The deformations and rotations at the end of each curved beam are calculated by using the Castigliano's theorem. By assuming that the beginning of each curved beam is fixed and loaded at the end by the appropriate loads, the solutions to the problem are given as follows:

In-plane bending:

The total strain energy due to bending of each curved beam is given by:

$$U_i = \int_{\alpha_i}^{\beta_i} M^2 R_i/2E_i I_{oi}\, d\phi \qquad \text{eq. (13)}$$

Deformations and rotations :

$$u_i = \partial U_i/\partial F_{xi} \quad ; \quad v_i = \partial U_i/\partial F_{yi} \quad ; \quad \phi_i = \partial U_i/\partial M_{zi} \qquad \text{eq. (14)}$$

By substituting eq. (13) in (14) and then performing the integration, one obtains:

Due to M_{zi} : $u_i = C_1 R_i \xi_1$; $v_i = C_1 R_i \xi_2$; $\phi_i = C_1 \xi_3$

Due to F_{xi} : $u_i = C_2 R_i \xi_4$; $v_i = C_2 R_i \xi_5$; $\phi_i = C_2 \xi_1$ eq. (15)

Due to F_{yi} : $u_i = C_3 R_i \xi_5$; $v_i = C_3 R_i \xi_6$; $\phi_i = C_3 \xi_2$

where $C_1 = M_{zi} R_i k_i/E_i I_i$; $C_2 = F_{xi} R_i^2 k_i/E_i I_i$; $C_3 = F_{yi} R_i^2 k_i/E_i I_i$; $A = \beta_i - \alpha_i = \xi_3$

$\xi_1 = A\sin\beta_i + \cos\beta_i - \cos\alpha_i$; $\xi_2 = -A\cos\beta_i + \sin\beta_i - \sin\alpha_i$; $\xi_4 = A\sin^2\beta_i + 2\sin\beta_i(\cos\beta_i - \cos\alpha_i) + \frac{1}{2}A$

$-\frac{1}{4}(\sin 2\beta_i - \sin 2\alpha_i)$; $\xi_5 = \cos(\alpha_i+\beta_i) - \cos 2\beta_i - \frac{1}{2}A\sin 2\beta_i + \frac{1}{4}(\cos 2\beta_i - \cos 2\alpha_i)$;
$\xi_6 = \frac{1}{2}A + \frac{1}{4}(\sin 2\beta_i - \sin 2\alpha_i) + A\cos^2\beta_i - 2\cos\beta_i(\sin\beta_i - \sin\alpha_i)$

Total deformations and rotations at the end of the (i+1)th curved beam :

$$\bar{u}_{i+1} = u_i + u_{i+1} + \Delta u_i \quad ; \quad \bar{v}_{i+1} = v_i + v_{i+1} + \Delta v_i \quad ; \quad \bar{\phi}_{i+1} = \phi_i + \phi_{i+1} \qquad \text{eq. (16)}$$

where $\Delta u_i = R_{i+1}\phi_i(\sin\beta_{i+1} - \sin\alpha_{i+1})$ and $\Delta v_i = R_{i+1}\phi_i(\cos\alpha_{i+1} - \cos\beta_{i+1})$

Out-of-plane bending:

In case of out-of-plane bending the total strain energy is given by:

$$U_i = \int_{\alpha_i}^{\beta_i} M^2 R_i / 2E_i I_{oi}\, d\phi + \int_{\alpha_i}^{\beta_i} T^2 R_i / 2G_i J_i\, d\phi \qquad \text{eq. (17)}$$

Deformation and rotations:

$$w_i = \partial U_i/\partial F_{zi} \quad ; \quad \omega_i = \partial U_i/\partial M_{ri} \quad ; \quad \psi_i = \partial U_i/\partial T_i \qquad \text{eq. (18)}$$

After substituting eq. (17) in (18) and then performing the integration, one obtains:

Due to M_{ri} : $w_i = C_4 R_i \xi_7$; $\omega_i = C_4 \xi_8$; $\psi_i = C_4 \xi_9$

Due to T_i : $w_i = C_5 R_i \xi_{10}$; $\omega_i = C_5 \xi_9$; $\psi_i = C_5 \xi_{11}$ eq. (19)

Due to F_{zi} : $w_i = C_6 R_i \xi_{12}$; $\omega_i = C_6 \xi_7$; $\psi_i = C_6 \xi_{10}$

where $C_4 = M_{ri} R_i k_i / E_i I_i$; $C_5 = T_i R_i k_i / E_i I_i$; $C_6 = F_{zi} R_i k_i / E_i I_i$; $B = (1+\mu)/k_i$;
$\xi_7 = \frac{1}{2}(B-1)\sin^2 A - B(1-\cos A)$; $\xi_8 = \frac{1}{2}A(1+B) + \frac{1}{4}(1-B)\sin 2A$; $\xi_9 = \frac{1}{2}(1-B)\sin^2 A$; $\xi_{10} = -\frac{1}{2}A(1+B)$
$+\frac{1}{4}(1-B)\sin 2A + B\sin A$; $\xi_{11} = \frac{1}{2}A(1+B) + \frac{1}{4}(B-1)\sin 2A$; $\xi_{12} = \frac{1}{2}A(1+3B) - \frac{1}{4}(1-B)\sin 2A - 2B\sin A$

Total deformation and rotations at the end of the (i+1)th curved beam:

$$\begin{aligned}
\bar{w}_{i+1} &= w_i + w_{i+1} - \omega_i R_{i+1}\sin(\beta_{i+1} - \alpha_{i+1}) + \psi_i R_{i+1}\{1 - \cos(\beta_{i+1} - \alpha_{i+1})\} \\
\bar{\omega}_{i+1} &= \omega_{i+1} + \omega_i \cos(\beta_{i+1} - \alpha_{i+1}) - \psi_i \sin(\beta_{i+1} - \alpha_{i+1}) \qquad \text{eq. (20)} \\
\bar{\psi}_{i+1} &= \psi_{i+1} + \omega_i \sin(\beta_{i+1} - \alpha_{i+1}) + \psi_i \cos(\beta_{i+1} - \alpha_{i+1})
\end{aligned}$$

Numerical results

Based on the above expressions, the end deformations and rotations of the whole suction bend are predicted. Calculations are made by assuming that one end (at the pump side) of the suction bend is fixed and the other end loaded by unity forces and moments of 10,000 N and 10.000 Nm respectively. The numerical results are given in Table I.

3. Second Method: Three Dimensional Stress Analyses

In the first method the influences of the neighbouring segments on the stresses and flexibility are neglected. Due to these influences redistribution of the stresses and change in the flexibility obtained by the first method may be expected. To investigate these effects stress analyses based on the finite element method are carried out by using the computer program ASKA.

Modelling of the problem: Analyses are made for the symmetry one half of the suction bend. Modelling is done by using the thick shell element QUABC9. Brief description of this element and the mesh for the analyses are given in Fig. 3. Some remarks are given here on the application of QUABC9 for the considered analyses. The suction bend can be classified as a thin shell construction. If thin shells are treated by the element QUABC9 the applicability of this element is restricted. Application of this element for thin shells problems needs reduction of the number of integration points when setting up the stiffness matrix [10, 11]. The presented element QUABC9 in ASKA allowed the reduced integration technique (2x2 integration scheme) only for the transverse shear terms. For the analyses this reduced integration scheme in chosen.

Boundary conditions: All degrees of freedom at the beginning (transition to the pump) of the bend are suppressed. For the symmetrical plane of the bend the following degrees of

freedom are suppressed (see Fig. 1) :

In-plane bending and internal pressure : Symmetric conditions $v_2 = 0$ and $\alpha = 0$

Out-of-plane bending : Skew-symmetric conditions $v_1 = 0$; $v_3 = 0$ and $\beta = 0$

Numerical results: Presentation of the results is given in the form of distribution of the stress intensification factor S at cross section 1 to 4 as shown in Fig. 4 to 8. The appropriate end deformations and rotations are given in Table I.

4. Discussion of the Results

Stresses: In the case of internal pressure loading, the greatest deviation occurs at cross section 1 as shown in Fig. 4. This can be explained by the compatibility conditions at the junction toroidal to cylindrical shell (nozzle) and the fold at the extrados. Prediction of the maximum stress at this cross section using the formulas for complete torus gives 36 N/mm^2 at $\theta = 0$ (intrados) to 48 N/mm^2 at $\theta = 80^o$ obtained by the three dimensional analysis. However this stress is lower than the predicted maximum stress in the suction bend viz. at cross section 2 as shown in Fig. 4. In general it can be said that the first method will give conservative results.

For the in- and out-of-plane bending comparisons are made for cross section 1 to 4 as shown in Fig. 5 to 8. As was to be expected redistribution of the stresses predominantly occur at the part of the suction bend near the pump, this is shown in Fig. 5/7. This phenomenon is due to the fact that at this part most change in the curvatures and cross sections are present. The stress distribution at cross sections(e.g. cross section 4) where the curvature and cross section gradually change are almost similar for both method.

Due to the loading conditions at the suction bend's end complex loading will occur at each cross section. In the first method the analyses are based on pure bending of the cross section. The influence of the non-pure bending of a cross section on the stress distribution is investigated. This is done basing on the three dimensional stress analyses by combining the appropriate loads at the suction bend's end. The results for cross section 2 and 4 are shown in Fig. 9 to 12. As shown in Fig. 10 for in-plane bending the total shear force has no influence on the results for pure bending, but the total longitudinal force will give significant influence on the stress distribution, this depend on the ratio $F_\phi t/M_z$. In the case of out-of-plane bending the influence of the torsion and shear force on the stresses due to pure bending is shown in Fig. 11/12 for various ratios of $T/2M_r$ and $F_z t/M_r$.

Flexibility: Comparisons are made of the results obtained by the analytical method explained in 2.3 and the three dimensional finite element method. As shown in Table I adequate agreement between both methods is confirmed. Prediction of the flexibility by applying the analytical method tends to give more flexible results.

5. Summary of Conclusions

- Adequate agreement is confirmed between the results obtained by both methods.
- For design purposes adequate and economical prediction of the stresses and flexibility can be obtained by using the first method.
- In complex loading special attention must be paid to analytical calculation of the stresses at the cross sections where non-pure bending occured. In this case the stresses will considerably deviate from the pure bending-stresses depending on the ratios $F_\phi t/M_z$, $F_z t/M_r$ and $T/2M_r$. However in general it can be said that for internal pressure and pure or nearly pure bending, the stresses predicted by the first method are conservative.

- More flexible bend will be predicted by the analytical method.

Acknowledgments

This work is part of the research into the integrity of the suction bend of the primary sodium pump for the LMFBR-SNR 300 sponsored by Neratoom B.V. - The Hague, The Netherlands. The author wishes to express his appreciation to Neratoom B.V. for their permission to publish this paper.

References

[1] ASME Boiler and Pressure Vessel Code - Section III - 1974

[2] Kalnins, A., "Analysis of Shells of Revolution Subjected to Symmetrical and Non-symmetrical Loads", J. App. Mech., Vol. 31, Sept 1964.

[3] Von Karman. Th., "Ueber die Formänderung dunnwandiger Rohre", Z.V.D.I., 1911.

[4] Vigness, I., "Elastic Properties of Curved Tubes", Trans. ASME Vol. 65, 1943.

[5] Turner, C.E. and Ford, H., "Examination of the Theories for Calculating the Stresses in Pipe Bends Subjected to In-plane Bending", Proc. Inst. Mech. Eng. 171,1957.

[6] Dodge, W.G. and Moore, S.E., "Stress Indices and Flexibility Factors for Moment Loadings on Elbows and Curved Pipe", WRC Bulletin 179.

[7] Pardue, T.E. and Vigness, I., "Properties of Thin Walled Curved Tubes of Short Bend Radius", Trans ASME, Jan. 1951.

[8] Gross, N., "Experiments on Short Radius Pipe Bends", Proc. Inst. Mech. Eng. 1(B), 1952-53.

[9] Rodabaugh, E.C. and George, H.H., "Effect of Internal Pressure on Flexibility and Stress Intensification Factors of Curved Pipe or Welding Elbows", Trans. ASME, 79,1957.

[10] Zienkiewicz, O.C., Taylor, R.L., Too, J.M., "Reduced Integration Technique in General Analysis of Plates and Shells", Int. J. Num. Math. Eng. Vol 3-1971

[11] "Thick shell Elements" - ISD-Report ASKA UM214.

TABLE I "END DEFORMATIONS-ROTATIONS OF THE SUCTION BEND"

ASKA				ANALYTIC			
u	w	ψ		u	w	ψ	Load
1.35	-1.15	-1.17 10^{-1}		1.58	-1.50	-1.33 10^{-1}	F_x
-1.13	1.15	0.94 10^{-1}		-1.50	1.85	1.23 10^{-1}	F_y
-1.16	0.95	1.10 10^{0}		-1.27	1.26	1.22 10^{0}	N_z
v	u	ψ		v	u	ψ	Load
1.04	-3.60 10^{-4}	-5.23 10^{-4}		1.05	-4.16 10^{-4}	-6.42 10^{-4}	F_z
0.36	-4.54 10^{-4}	1.26 10^{-4}		0.33	-6.65 10^{-4}	-0.60 10^{-4}	M_x
0.69	1.10 10^{0}	6.19 10^{-4}		-0.73	0.60 10^{0}	6.64 10^{-4}	M_y

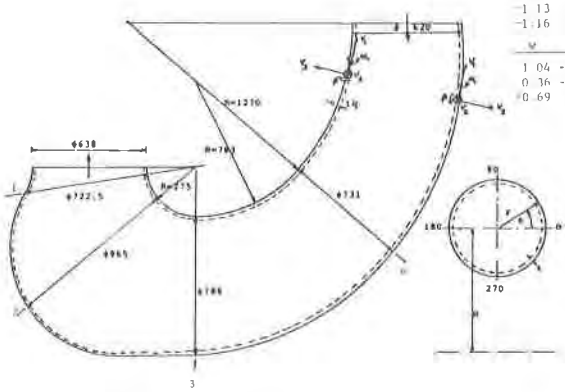

1,2,3 and 4 designate cross sections

FIG 1 SUCTION BEND'S GEOMETRY AND POSITION OF THE CROSS SECTION

Beam	R (mm)	r (mm)	t (mm)	α	β	h
1	613	331	14	0.0	87.20	2
2	759	477	14	87	90.0	32.0
3	1148	328	14	90.0	138.5	14.1
4	1616	339	14	138.5	180.0	8.0

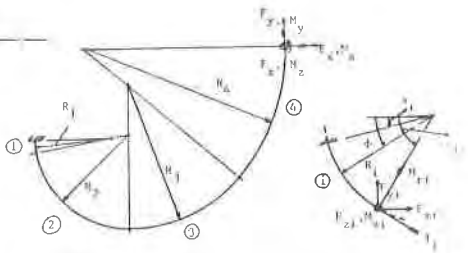

FIG 2 CURVED BEAMS ASSEMBLY FOR DETERMINING THE FLEXIBILITY

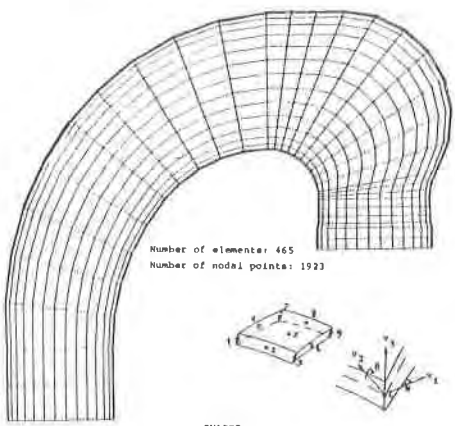

FIG 3 MESH FOR THE 3-DIMENSIONAL FINITE ELEMENT METHOD ANALYSIS

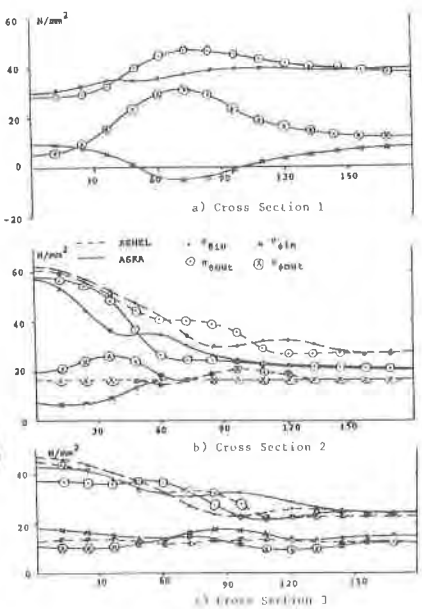

0° = INTRADOS 180° = EXTRADOS

FIG 4 STRESS DISTRIBUTION DUE TO INT PRESS 1 N/mm²

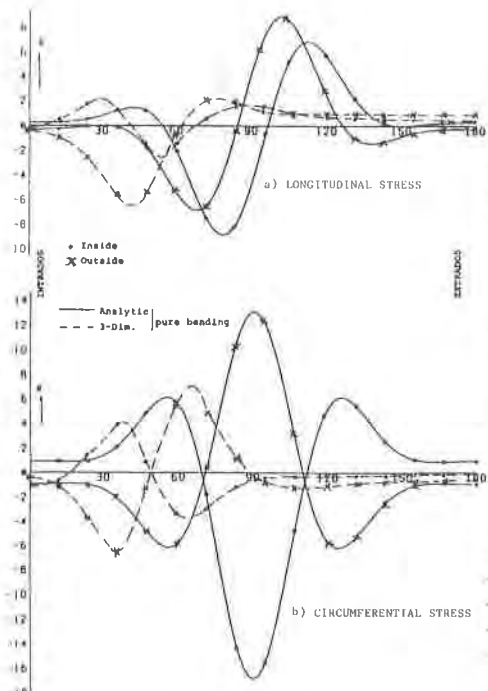

FIG 5 "IN-PLANE BENDING" STRESS INTENSIFICATION FACTOR AT CROSS SECTION 2

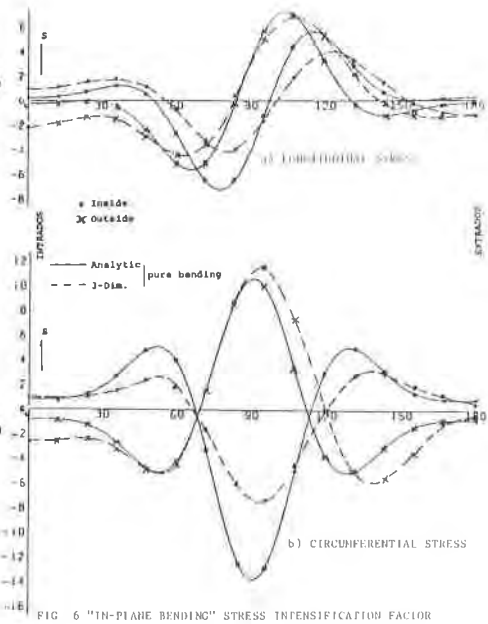

FIG 6 "IN-PLANE BENDING" STRESS INTENSIFICATION FACTOR AT CROSS SECTION 3

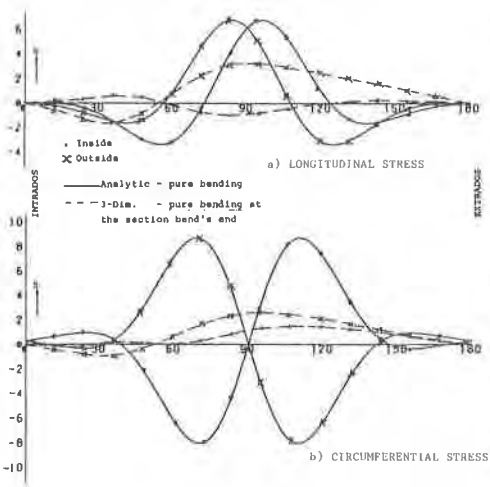

FIG 7 "OUT-OF-PLANE BENDING" STRESS INTENSIFICATION FACTOR AT CROSS SECTION 1

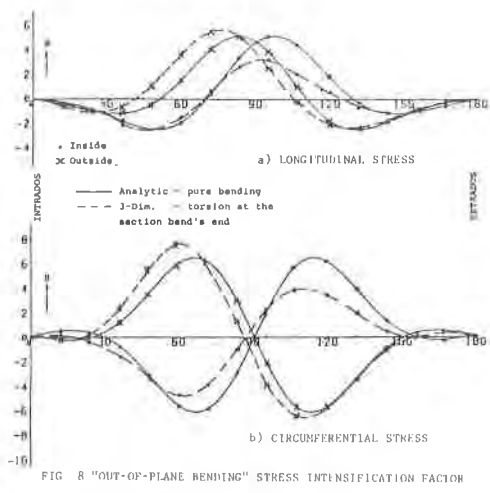

FIG 8 "OUT-OF-PLANE BENDING" STRESS INTENSIFICATION FACTOR AT CROSS SECTION 4

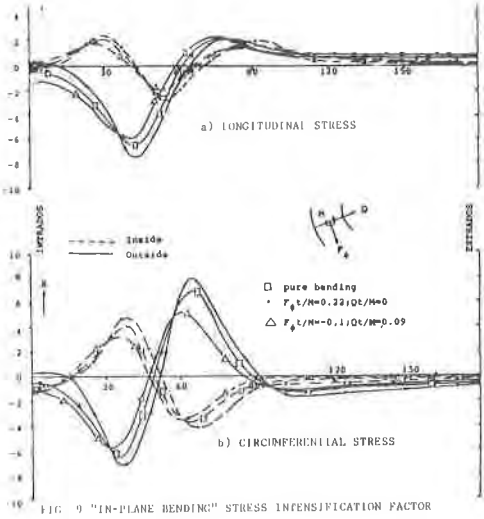

FIG. 9 "IN-PLANE BENDING" STRESS INTENSIFICATION FACTOR AT CROSS SECTION 2

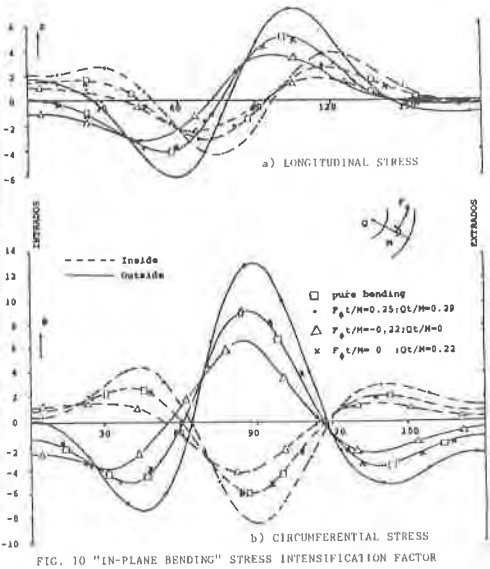

FIG. 10 "IN-PLANE BENDING" STRESS INTENSIFICATION FACTOR AT CROSS SECTION 4

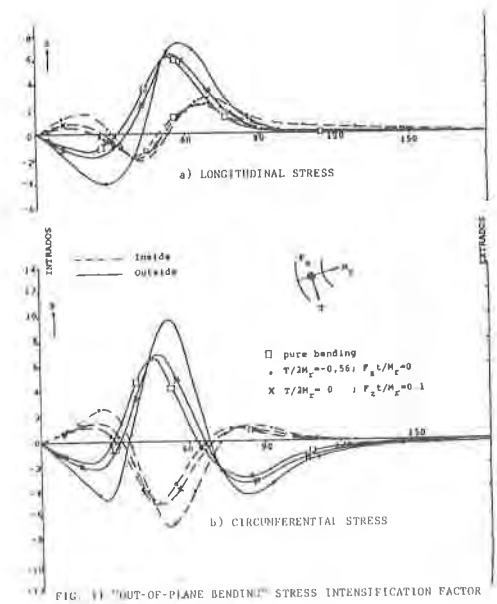

FIG. 11 "OUT-OF-PLANE BENDING" STRESS INTENSIFICATION FACTOR AT CROSS SECTION 2

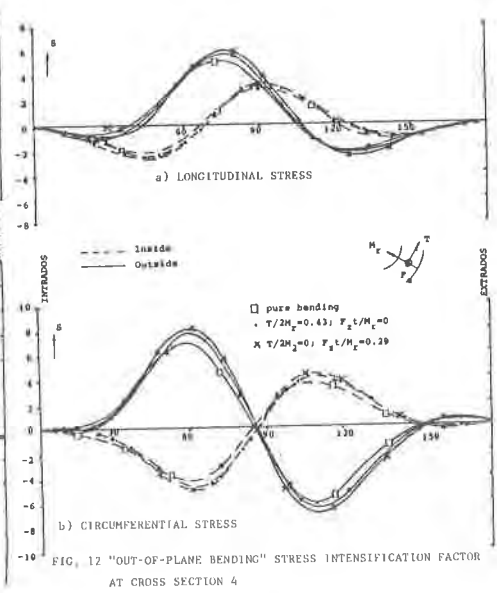

FIG. 12 "OUT-OF-PLANE BENDING" STRESS INTENSIFICATION FACTOR AT CROSS SECTION 4